Effect of Spin-Surface Crossing on the Kinetics of Sequential Ligation of Ru^+ with Ammonia in the Gas Phase at Room Temperature

S. I. Gorelsky, V. V. Lavrov, G. K. Koyanagi, A. C. Hopkinson, and D. K. Bohme*

Department of Chemistry, Centre for Research in Mass Spectrometry and Centre for Research in Earth and Space Science, York University, Toronto, Ontario, Canada M3J 1P3

Received: January 18, 2001; In Final Form: July 12, 2001

Gas-phase measurements of the kinetics for the sequential ligation of Ru^+ with ammonia at room temperature show an anomalous rise in the rate of addition of the fourth ammonia ligand unlike in the ammonia-ligation kinetics of Mg^+, Fe^+, and Ag^+. The measurements were conducted with an inductively-coupled plasma/selected-ion flow tube (ICP/SIFT) tandem mass spectrometer. B3LYP/ DZVP calculations of ligation free energies for the ammonia ligation of ground-state $Ru^+(^4F)$ and of $Ru^+(^2D)$ indicate a reversal in the relative ligation free energy that favors the ligation of $Ru^+(^2D)$ in the addition of the fourth ammonia ligand. Since the rate of ligation is dependent on the free energy of ligation, these results are consistent with the occurrence of a spin surface-crossing in the sequential ligation of $Ru^+(^4F)$ with ammonia.

Introduction

Spin surface-crossing effects are known to be important in determining the outcome of chemical reactions.[1,2] This has been emphasized recently by Schröder, Shaik, and Schwarz in a review of two-state spin reactivity in organometallic chemical-reaction pathways involving more than one spin surface.[1] Case studies involving transition metals are discussed by these authors that illustrate the operation of spin surface-crossing effects in determining reaction mechanisms, rate coefficients, branching ratios, and temperature dependencies for organometallic reactions in the gas phase. Also, in measurements of metal-ion ligation energies, Armentrout and co-workers[3] have interpreted observed variations in sequential energies of ligation in terms of changes in the spin of the ligated ions. Here we report a combined experimental and theoretical study that provides evidence for the participation of more than a single spin surface in the sequential ligation of Ru^+ with ammonia in the gas phase at room temperature. We attribute an observed change in the sequential rate of ligation to the occurrence of a spin-surface crossing and suggest that spin-surface crossing effects may operate more generally on the kinetics of ligation of other atomic metal ions.

Experimental Method

The kinetics for the ligation of Ru^+ with ammonia was investigated with an inductively-coupled plasma/selected-ion flow tube (ICP/SIFT) mass spectrometer. Ru^+ ions were generated in an ICP source from a nebulized ruthenium-salt solution. This solution had a concentration of 5 ppm Ru (stabilized in 2% HCl). Ions derived from the plasma were introduced into the SIFT through an atmosphere/vacuum interface, selected with a quadrupole mass filter, and injected into flowing helium gas. The ammonia was added into the flow tube further downstream up to the maximum amount measurable. Both reactant and product ions were sampled at the end of the reaction region and analyzed with a second quadrupole mass filter. The ICP ion source and interface have been described previously,[4,5] as has the basic SIFT instrument.[6,7]

Helium was used as the SIFT buffer gas at 0.35 ± 0.01 Torr. The flow tube temperature was 296 ± 2 K. The selected Ru^+ ions that entered the flow tube were allowed to thermalize by collisions with He (ca. 4×10^5 collisions) prior to entering the reaction region further downstream at the point of addition of the ammonia reagent gas. The neutral reactant, ammonia, was anhydrous grade, with a minimum purity of 99.99%, supplied by Matheson Gas Products.

At a nominal plasma temperature of 5000 K the Ru^+ ions emerge primarily in the electronic states ^4F:^4P:^6D:^2G:^2P:^2D:^2H at electronic energies of 0, 1.023, 1.134, 1.346, 1.606, 1.807, and 1.817 eV, respectively, in a proportion of 1:0.097:0.096:0.029:0.029:0.009:0.010, respectively. The energies of the electronic states and the electronic-state population distribution were computed using spectroscopic data tabulated in ref 8 and assuming that the ions are thermalized at the nominal plasma temperature. In the experiments reported here there was no obvious indication of the presence of more than 1 electronic state of Ru^+ in the reaction region: in the reaction with ammonia the observed decay of Ru^+ was linear over 1 order of magnitude. The calculated electronic state populations indicate that at least 79% of the Ru^+ ions are in their ground ^4F state and a total of 87% are in quartet states. The remaining 13% would introduce noticeable curvature into the measured decay over 1 order of magnitude if they reacted with rate coefficients different by more than about a factor of 2. The ions emerging from the plasma may experience both radiative electronic-state relaxation and collisional electronic-state relaxation prior to entering the reaction region. The latter may happen with argon as the extracted plasma cools upon sampling and then by collisions with He atoms in the flow tube prior to the reaction region, but the extent of this is not known. There is the (remote) possibility that the reactivity of Ru^+ with ammonia is essentially the same for all the populated electronic states. The collisions with He ensure that the Ru^+ ions reach a translational temperature equal to the tube temperature of 296 ± 2 K prior to entering the reaction region.

The rate coefficient for the primary addition reaction was determined from the measured semilogarithmic decay of the reactant ion as a function of the flow of the added reagent gas.[6,7]

* Corresponding author. E-mail: dkbohme@yorku.ca.

10.1021/jp010205+ CCC: $20.00
Published on Web 09/20/2001

TABLE 1: Geometries and Dipole Moments of $Ru(NH_3)_n^+$ at B3LYP/DZVP[a]

ion	spin *S*	geometry	point group	Ru−N dists, Å	N−Ru−N angle, deg	dipole moment, D
$Ru(NH_3)^+$	1/2	linear	C_s	2.169[b]		2.6[a]
	3/2	**linear**	C_{3v}	**2.234**		**2.2**
	5/2	linear	C_{3v}	2.377		4.3
$Ru(NH_3)_2^+$	1/2	bent	C_{2v}	2.158	96.3	3.4
	3/2	**bent**	C_{2v}	**2.247**	**172.1**	**0.3**
	5/2			**dissociates**		
$Ru(NH_3)_3^+$	1/2	T-shaped	C_s	2.168, 2.225(2)	91.9, 92.8	2.0
	3/2	**pyramidal**	C_{3v}	**2.334−2.342**	**117.7−117.8**	**1.0**
	3/2	T-shaped	C_s	2.469, 2.286(2)	95.1, 96.0	1.9
$Ru(NH_3)_4^+$	**1/2**	**square planar**	C_{4h}	**2.232**	**90.0**	**0.0**
	3/2	tetrahedral	T_d	2.394	109.5	0.0
$Ru(NH_3)_5^+$	**1/2**	**square pyramidal**	C_1	**2.243(4), 2.692**	**92.1−92.5**	**1.5**
	3/2	solvated tetrahedral	C_s	2.358−2.405	108.1−109.2	0.9

[a] The lowest energy species are shown in boldface. [b] S^2 before annihilation 1.4192, after 0.7509.

TABLE 2: Total Energies, Gibbs Free Energies (298 K), Unscaled Zero-Point Energies, and Entropies of $Ru(NH_3)_n^+$ at B3LYP/DZVP[a]

ion	spin *S*	tot. energy (hartrees)	G_{298K} (hartrees)	ZPE (hartrees)	entropy (cal K^{-1} mol^{-1})
NH_3	0	−56.564 04	−56.548 56	0.034 56	48.2
Ru^+	1/2	−4442.865 30	−4442.882 49	0	41.2
	3/2	**−4442.926 29**	**−4442.944 14**	**0**	**42.5**
	5/2	−4442.843 19	−4442.861 42	0	43.3
$Ru(NH_3)^+$	1/2	−4499.539 63[a]	−4499.527 16[a]	0.038 75[b]	64.4[a]
	3/2	**−4499.566 30**	**−4499.554 88**	**0.038 46**	**66.2**
	5/2	−4499.480 88	−4499.470 89	0.037 62	67.8
$Ru(NH_3)_2^+$	1/2	−4556.171 80	−4556.125 90	0.078 13	83.1
	3/2	**−4556.196 77**	**−4556.151 09**	**0.077 44**	**82.6**
	5/2		dissociates		
$Ru(NH_3)_3^+$	1/2	−4612.795 85	−4612.714 41	0.117 25	96.5
C_{3v}	**3/2**	**−4612.797 73**	**−4612.720 48**	**0.115 25**	**102.9**
C_s	3/2	−4612.786 09	−4612.709 55	0.115 34	104.6
$Ru(NH_3)_4^+$	**1/2**	**−4669.410 60**	**−4669.293 03**	**0.156 22**	**108.2**
	3/2	−4669.392 39	−4669.279 62	0.153 52	115.0
$Ru(NH_3)_5^+$	**1/2**	**−4725.984 03**	**−4725.840 32**	**0.191 75**	**137.6**
	3/2	−4725.972 53	−4725.832 66	0.189 83	143.4

[a] The lowest energy species are shown in boldface. [b] S^2 before annihilation 1.4192, after 0.7509.

Higher-order rate coefficients were deduced from a fit to the observed ammonia cluster-ion profiles with solutions to the differential equations appropriate to sequential ligation kinetics.

Computational Methods

All molecular orbital calculations were performed using Gaussian 98.[9] Structure optimizations were carried out using the density functional theory (DFT) with Becke's three-parameter hybrid functional[10,11] with LYP correlation functional[12,13] (B3LYP). The double-ζ split-valence polarization basis set DZVP[14,15] was used for structure optimizations on all ions. All critical points were characterized by harmonic frequency calculations. Calculated structural and thermodynamic properties of $Ru(NH_3)_n^+$ ions are presented in Tables 1−3.

Results and Discussion

Experimental Results. Observations of the sequential ligation of Ru^+ with ammonia according to reaction 1 are shown in Figure 1. Up to five molecules of ammonia were seen to add to Ru^+ under SIFT conditions. The addition is presumed to occur by collisional rather than radiative association with He acting as the stabilizing third body. Effective bimolecular rate coefficients, k_n, were determined from the initial Ru^+ ion semilogarithmic decay and by curve fitting the $Ru(NH_3)_n^+$ ion profiles in Figure 1 with solutions to the differential equations appropriate to sequential ligation kinetics: $k_1 = 7.7 \times 10^{-12}$, $k_2 = 3.6 \times 10^{-10}$, $k_3 = 5.3 \times 10^{-11}$, $k_4 = 3.6 \times 10^{-10}$, and $k_5 = 2.0 \times 10^{-12}$ cm^3 $molecule^{-1}$ s^{-1}. The kinetic model that was used to fit the data and extract rate coefficients assumes irreversible consecutive addition reactions. Our experience has been that this assumption is justified under our operating conditions at room temperature for addition reactions with standard free-energy changes more negative than −9 kcal mol^{-1}. The results of our calculations indicate that this condition is met for all but the fifth addition for which the free energy of ligation is positive. Also, we checked for the occurrence of equilibrium with product-to-reactant ion-signal ratio plots but these were not suggestive of equilibrium. The rapid fourth addition is rate-limited by the formation of the third adduct. The last addition

TABLE 3: Enthalpies, Entropies, and Gibbs Free Energies of Formation of $Ru(NH_3)_n^+$, $Ru^+(^4F)$, + nNH_3 → $Ru(NH_3)_n^+$, at the B3LYP/DZVP Level[a]

n	spin *S*	$\Delta H_{f,298K}$ (kcal mol^{-1})	$\Delta S_{f,298K}$ (cal mol^{-1} K^{-1})	$\Delta G_{f,298K}$ (kcal mol^{-1})
1	1/2	−29.5[b]	−26.3[b]	−21.5[b]
1	**3/2**	**−46.4**	**−24.5**	**−38.9**
1	5/2	+6.8	−22.9	+13.7
2	1/2	−69.8	−55.7	−53.0
2	**3/2**	**−85.8**	**−56.2**	**−68.8**
3	1/2	−105.2	−90.5	−78.1
3 (C_{3v})	**3/2**	**−107.2**	**−84.2**	**−82.1**
3 (C_s)	3/2	−99.8	−82.4	−75.0
4	**1/2**	**−135.0**	**−127.0**	**−96.9**
4	3/2	−124.5	−120.1	−88.5
5	**1/2**	**−139.8**	**−145.7**	**−96.1**
5	3/2	−133.2	−140.0	−91.3

[a] The lowest energy species are shown in boldface. [b] S^2 before annihilation 1.4192, after 0.7509.

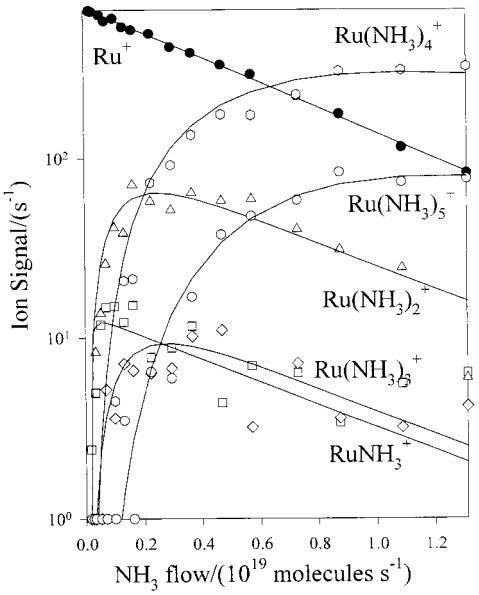

Figure 1. Ion profiles obtained with the ICP/SIFT apparatus for the chemistry initiated by Ru^+ with ammonia in helium buffer gas at 0.35 Torr and 296 ± 2 K.

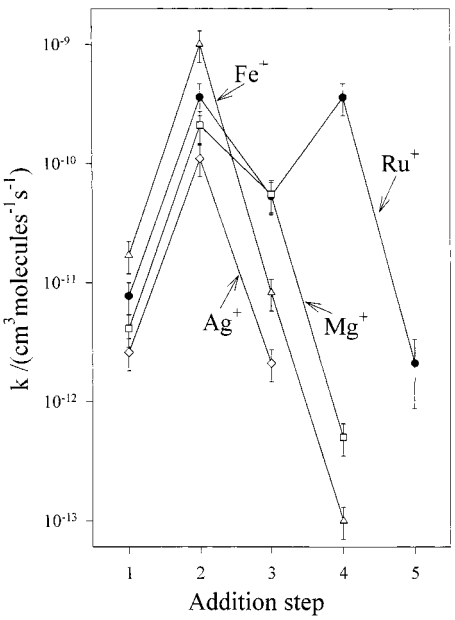

Figure 2. Measured variation in the apparent bimolecular rate coefficient for ammonia ligation of Ag^+, Fe^+, Mg^+, and Ru^+ in helium buffer gas (at 0.35 Torr and 296 ± 2 K) with the number, *n*, of the ammonia ligand added in the reaction $M(NH_3)_{n-1}^+ + NH_3 \rightarrow M(NH_3)_n^+$. The error bars represent the combined estimated error due to the experimental and the fitting procedures.

may indeed approach equilibrium but the $Ru(NH_3)_5^+/Ru(NH_3)_4^+$ ion-signal ratio plot did not indicate this: the ion-signal ratio should become linearly dependent on flow, but it becomes nearly constant instead, perhaps due to further solvation with another ammonia molecule. $Ru(NH_3)_6^+$ was not observed but this may be due to weak bonding of the 6th ammonia molecule and its removal either thermally or upon sampling.

$$Ru(NH_3)_{n-1}^+ + NH_3 \rightarrow Ru(NH_3)_n^+ \qquad (1)$$

The computational procedure used to fit the experimental data is based on finding the hypersurface that minimizes the sum of squared deviations between the model and experimental points. It requires the rate coefficient used for fitting to be constrained usually within ±10%. Too loose a constraint, in practice beyond ±20−30%, leads to divergence causing an infinite loop or yields physically meaningless values due to round-off errors in the exponent function. We estimate a total uncertainty in the rate coefficients to be ±30% of their reported (most probable) values. The total estimated uncertainty is a combination of experimental error and the uncertainties associated with the fitting procedure.

The variation in the rate coefficient with the number of added ligands is shown in Figure 2 together with those measured previously in our laboratory for the ligation reactions of Mg^+, Ag^+, and Fe^+ with NH_3 under similar operating conditions.[16,17] Clearly the sequential ligation kinetics for Ru^+ are unique in that they display a minimum in the rate coefficient for sequential ligation (for the addition of the third ligand).

Theoretical Results. (a) Structural Details. Figure 3 displays structural details computed for the ligated $Ru(NH_3)_n^+$ ions for $n = 1-5$. The Ru−N bond lengths in the low-spin (doublet) complexes are always shorter than those in high-spin (quartet) complexes with the same number of ammonia ligands. This is attributed to the availability of one valence shell d orbital in the low-spin complexes, whereas in the high-spin complexes bonding involves the 5s and 5p orbitals.

Calculations showed that only one complex of Ru^+ with orbital occupancy $4d^65s^1$ (a ^6D state) forms a complex, the monoadduct, that is stable toward dissociation.

High-Spin Complexes. The gross features of structures of complexes of $Ru^+(^4F)$ with NH_3 can be easily understood in terms of a simple sp^n hybridization scheme. The bond distances increase with the number of ligands from 2.234 Å in $Ru(NH_3)^+$ to 2.394 Å in $Ru(NH_3)_4^+$, consistent with a picture of increasing amounts of p character.

$Ru(NH_3)_2^+$ has a bond angle of 172.1°, close to the linear angle expected for an ideal sp-hybridized metal ion. The unusual feature of this ion is that the two NH_3 molecules adopt an eclipsed conformation. Optimization of the linear structure in which the two NH_3 molecules are staggered resulted in a structure at a first-order saddle point, 2.8 kcal mol^{-1} above the eclipsed conformation.

Two structures, both at minima, were located on the high-spin $Ru(NH_3)_3^+$ potential energy surface. The structure with the lowest energy is pyramidal, but the out-of-plane angle is small. This complex is best described as having a sp^2-hybridized Ru atom. The other isomer with the same multiplicity is 7.4 kcal mol^{-1} higher in energy and has a T-shape. This can be described by dsp hybridization of the ruthenium, a scheme that requires one of the d electrons to be promoted to a 5p orbital.

$Ru(NH_3)_4^+$ is tetrahedral and has a Ru atom that is sp^3 hybridized. Attempts to optimize a complex of $Ru^+(^4F)$ with five NH_3 molecules in direct coordination with the metal ion all resulted in rearrangement to the tetrahedrally substituted ion with the additional NH_3 molecule attached to a ligating NH_3 through a hydrogen bond. Comparison of the bond distances in the solvated ion with those in the nonsolvated ion shows that solvation results in a slight shortening (by 0.037 Å) of the Ru−N bond for the solvated ligand and even smaller lengthenings of the other Ru−N distances.

Low-Spin Complexes. Orbitals available for bonding in doublet Ru^+ are one 4d, the 5s, and three 5p orbitals. All the hybridization schemes proposed here include using the d orbital.

$Ru(NH_3)_2^+$ has a bond angle of 96.3° and is best described as containing an sd-hybridized metal ion. $Ru(NH_3)_3^+$ is T-shaped with bond angles close to 90° and is essentially dsp hybridized.

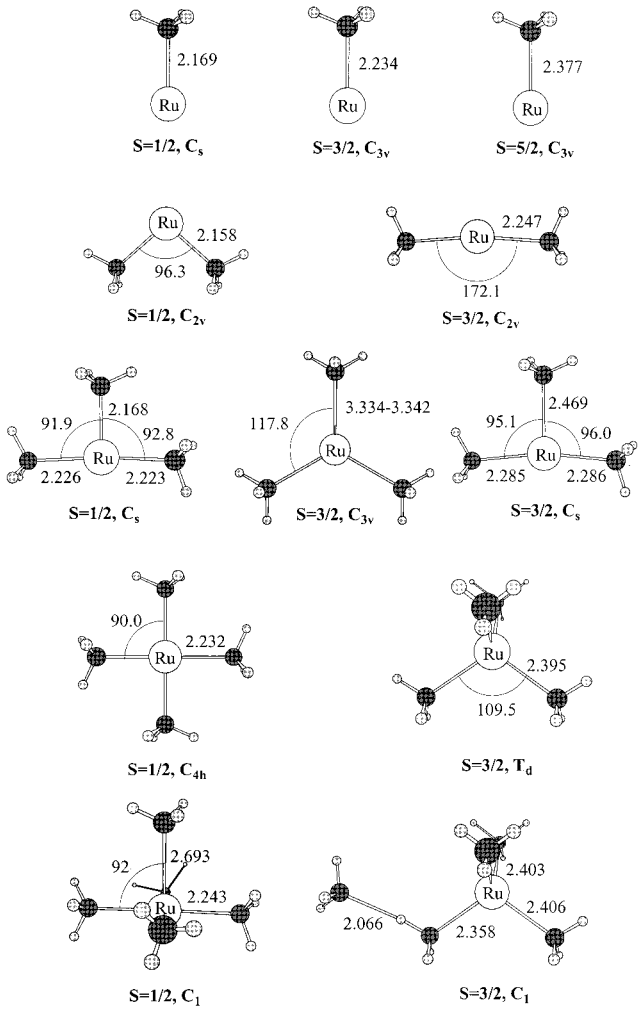

Figure 3. Geometries computed for $Ru(NH_3)_n^+$ ions with n up to 5. Bond lengths are given in Å, and angles, in deg.

The Ru−N bond distances in the low-spin complexes $Ru(NH_3)_n^+$, where $n = 1-3$, are in the range 2.158−2.169 Å, the shortest distances in any of these complexes.

$Ru(NH_3)_4^+$ is square planar (dsp^2 hybridization), and the $Ru(NH_3)_5^+$ complex is square pyramidal (dsp^3 hybridization). The bonds in the plane of the five coordinate structure (2.243 Å) are slightly longer than in the square planar four coordinate complex (2.232 Å). The axial bond in the five coordinate structure (2.679 Å) is much longer than any other Ru−N bond encountered in any of the other complexes studied here. We attribute this to the high amount of p character required to describe the bonding along this direction.

(b) Energetics. In its outer shell, Ru^+ has an orbital occupancy of $4d^7$ and the ground electronic state is a high-spin quartet (^4F). At B3LYP/DZVP the low-spin doublet (^2D) state is calculated to be 38.3 kcal mol^{-1} higher in energy. Reaction of the ion in the ^4F state with NH_3 molecule is exothermic by 46.4 kcal mol^{-1} ($\Delta H = -46.4$ kcal mol^{-1}). Subsequent sequential additions of NH_3 molecules to $Ru(NH_3)^+$ are exothermic by 39.4, 21.4, 17.3, and 8.7 kcal mol^{-1}, respectively. In this respect $Ru^+(^4F)$ behaves similarly to Ag^+ (orbital occupancy $4d^{10}$, electronic state ^1S): additions of the first two NH_3 molecules to Ag^+ are exothermic by around 38 kcal mol^{-1}, the next two are around 13 kcal mol^{-1}, and subsequent additions involving direct coordination have very low exothermicities and with free energies for the formation reaction close to zero (see Table 3 in ref 17).

The exothermicities of the reactions of doublet Ru^+ with NH_3 molecules do not follow the same trend. The first addition has a large exothermicity (67.8 kcal mol^{-1}), and the next three sequential additions all have higher exothermicities than addition reactions for the corresponding ions in the quartet state. Addition of the second NH_3 is exothermic by 40.3 kcal mol^{-1}, and the third and fourth additions are of comparable energies (35.4 and 29.8 kcal mol^{-1}). Addition of a fifth NH_3 molecule is very weakly exothermic (by 4.8 kcal mol^{-1}).

The higher exothermicities of the addition reactions of the low-spin $Ru(NH_3)_n^+$ complexes results in the doublets becoming lower in energy than high-spin complexes when $n > 3$. For $n = 3$, two high-spin complexes of $Ru(NH_3)_3^+$ were located 7.4 kcal mol^{-1} apart on the potential energy surface. The ion with the lower energy, essentially a trigonal planar structure, is at the global minimum, 2 kcal mol^{-1} lower than the low spin T-shaped ion.

Discussion

We have now measured the kinetics for sequential ammonia ligation under SIFT conditions for the atomic ions $Mg^+(^2S)$,[16] $Ag^+(^1S)$,[17] and $Fe^+(^6D)$[16] in addition to $Ru^+(^4F)$. The comparison shown in Figure 2 clearly indicates that the oscillating behavior of the rate of Ru^+ ligation with the number of ligands is unique and requires an explanation.

The ligation of Ru^+ with ammonia under our SIFT experimental conditions is expected to proceed by termolecular association (with He acting as the third body) so that its rate will be determined by the lifetime of the intermediate complex. This is so since *gas-phase* ligation at moderate pressures and room-temperature proceeds in two steps: the formation of a transient intermediate $(ML_{n+1}^+)^*$ (where M^+ is the metal ion and L is a ligand), reaction 2, and collisional stabilization, reaction 3. The lifetime of the transient intermediate against dissociation back to reactants is dependent both on the degrees of freedom effective in intramolecular energy redisposition in the transient intermediate $(ML_{n+1}^+)^*$ and on its attractive well depth, $D(ML_n^+ - L)$, viz., the ligation energy of ML_n^+. Application of unimolecular decomposition theory for the back-dissociation of the transient intermediate together with a steady-state analysis of this two-step mechanism indicates that the effective bimolecular rate coefficient for ligation $k \propto D^{s-1}$, where s is the number of degrees of freedom effective in intramolecular energy redisposition.[17] So the initial rise in rate observed for the second step in ammonia ligation, a common feature in Figure 2 for all four atomic ions investigated, can be attributed to the increase in degrees of freedom associated with the addition of the first ligand. We previously have attributed the subsequent drop in the rate of ligation for Mg^+, Ag^+, and Fe^+ to a decrease in the ligation free energy.[15,16] The decrease in ligation energy was substantiated theoretically for ammonia ligation of Mg^+ and Ag^+.[16] The calculations reported here also indicate a drop in the ligation free energy with increasing ammonia ligation for both the $Ru^+(^4F)$ and $Ru^+(^2D)$ electronic states: −38.9, −29.9, −13.3, −6.4, and −2.8 kcal mol^{-1} for the ligation of $Ru^+(^4F)$; −21.5, −31.5, −25.1, −18.8, and +0.8 kcal mol^{-1} for the ligation of $Ru^+(^2D)$.

$$ML_n^+ + L \rightarrow (ML_{n+1}^+)^* \quad (2)$$

$$(ML_{n+1}^+)^* + He \rightarrow ML_{n+1}^+ + He^* \quad (3)$$

These patterns in ligation free energy are shown in Figure 4, and it is clear that there is an intersection in the spin quartet

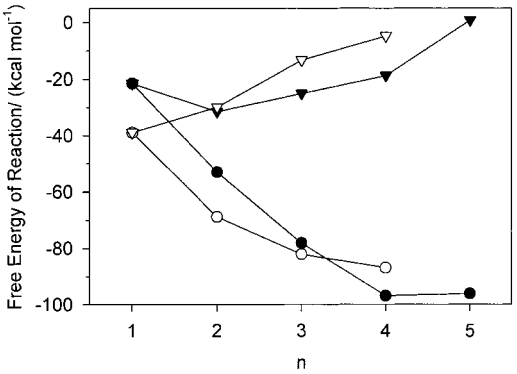

Figure 4. Computed free energies for reactions of the type $Ru^+ + nNH_3 \rightarrow Ru(NH_3)_n^+$ with n up to 5. Cumulative free energies are given as circles, and sequential free energies are given as triangles. The open circles and triangles represent values for spin quartet electronic states of $Ru(NH_3)_n^+$, and the solid circles and triangles represent those for spin doublet states.

and spin doublet free energies of ligation so that a crossing from the quartet to the doublet spin surfaces becomes possible. The ligation free energy for the addition of the fourth ligand to the doublet, -18.8 kcal mol^{-1}, is substantially larger than that to the quartet, -6.4 kcal mol^{-1}. Furthermore, and more significantly, it is substantially larger than the ligation free energy for the addition of the third ligand to the quartet, -13.3 kcal mol^{-1}. So the rise in the rate of ligation for the addition of the fourth ammonia molecule, expected with a rise in ligation free energy, is consistent with the occurrence of a crossing from the quartet to the doublet energy surface. The actual extent of the proposed spin change is not known; it may not be complete, but we suggest that the increase in the rate constant by nearly 1 order of magnitude points to it being nearly so.

Acknowledgment. Continued financial support from the Natural Sciences and Engineering Research Council of Canada is greatly appreciated. Also, we acknowledge support from the National Research Council, the Natural Sciences and Engineering Research Council, and MDS SCIEX in the form of a Research Partnership grant.

References and Notes

(1) Schröder, D.; Shaik, S. H.; Schwarz, H. *Acc. Chem. Res.* **2000**, *33*, 139.

(2) Armentrout, P. B. *Science* **1991**, *251*, 175.

(3) See, for example: Schultz, R. H.; Armentrout, P. B. *J. Phys. Chem.* **1993**, *97*, 596.

(4) Koyanagi, G. K.; Lavrov, V. V.; Baranov, V.; Bandura, D.; Tanner, S.; McLaren, J. W.; Bohme, D. K. *Int. J. Mass Spectrom.* **2000**, *194*, L1.

(5) Koyanagi, G. K.; Baranov, V.; Tanner, S.; Bohme, D. K *J. Anal. At. Spectrom.* **2000**, *15*, 1207.

(6) MacKay, G. I.; Vlachos, G. D.; Bohme, D. K.; Schiff, H. I. *Int. J. Mass Spectrom. Ion Phys.* **1980**, *36*, 259.

(7) Raksit, A. B.: Bohme, D. *Int. J. Mass Spectrom. Ion Phys.* **1983**, *55*, 69.

(8) Moore, C. E. *Atomic energy levels as derived from the analysis of optical spectra*; U.S. Bureau of Standards: Washington, DC, 1971; Vol. II.

(9) Frisch, M. J.; Trucks, G. W.; Schlegel, H. B.; Scuseria, G. E.; Robb, M. A.; Cheeseman, J. R.; Zakrzewski, V. G.; Montgomery, J. A., Jr.; Stratmann, R. E.; Burant, J. C.; Dapprich, S.; Millam, J. M.; Daniels, A. D.; Kudin, K. N.; Strain, M. C.; Farkas, O.; Tomasi, J.; Barone, V.; Cossi, M.; Cammi, R.; Mennucci, B.; Pomelli, C.; Adamo, C.; Clifford, S.; Ochterski, J.; Petersson, G. A.; Ayala, P. Y.; Cui, Q.; Morokuma, K.; Malick, D. K.; Rabuck, A. D.; Raghavachari, K.; Foresman, J. B.; Cioslowski, J.; Ortiz, J. V.; Stefanov, B. B.; Liu, G.; Liashenko, A.; Piskorz, P.; Komaromi, I.; Gomperts, R.; Martin, R. L.; Fox, D. J.; Keith, T.; Al-Laham, M. A.; Peng, C. Y.; Nanayakkara, A.; Gonzalez, C.; Challacombe, M.; Gill, P. M. W.; Johnson, B. G.; Chen, W.; Wong, M. W.; Andres, J. L.; Head-Gordon, M.; Replogle, E. S.; Pople, J. A. *Gaussian 98*, revision A.7; Gaussian, Inc.: Pittsburgh, PA, 1998.

(10) Becke, A. D. *Phys. Rev.* A **1988**, *38*, 3098.

(11) Becke, A. D. *J. Chem. Phys.* **1993**, *93* 5648.

(12) Lee, C.; Yang, W.; Parr, R. G. *Phys. Rev. B* **1988**, *37*, 785.

(13) Miehlich, B.; Savin, A.; Stoll, H.; Preuss, H. *Chem. Phys. Lett.* **1989**, *157*, 200.

(14) Godbout, N.; Salahub, D. R.; Andzelm, J.; Wimmer, E. *Can. J. Chem.* **1992**, *70*, 560.

(15) Basis sets were obtained from the Extensible Computational Chemistry Environment Basis Set Database, Version 1.0, as developed and distributed by the Molecular Science Computing Facility, Environmental and Molecular Sciences Laboratory, which is part of the Pacific Northwest Laboratory, P.O. Box 999, Richland, WA 99352, and is funded by the U.S. Department of Energy. The Pacific Northwest Laboratory is a multiprogram laboratory operated by Battelle Memorial Institute for the U.S. Department of Energy under Contract DE-AC06−76RLO 1830. Contact David Feller or Karen Schuchardt for further information.

(16) Milburn, R.; Baranov, V. I., Hopkinson, A. C.; Bohme, D. K. *J. Phys. Chem. A* **1998**, *102*, 9803.

(17) Shoeib, T.; Milburn, R. K., Koyanagi, G. K.; Lavrov, V. V., Bohme, D. K.; Siu, K. W. M.; Hopkinson, A. C. *Int. J. Mass Spectrom.* **2000**, *201*, 87.

(18) See, for example: Tonkyn, R.; Ronan, M.; Weisshaar, J. C. *J. Phys. Chem.* **1988**, *92*, 92.